On the mix-mode fracture of carbon fibre/epoxy composites interleaved with various thermoplastic veils

Quan, Dong; Yue, Dongsheng; Ma, Yannan; Zhao, Guoqun; Alderliesten, René

DOI
10.1016/j.coco.2022.101230

Publication date
2022

Document Version
Final published version

Published in
Composites Communications

Composites Communications 33 (2022) 101230

Contents lists available at ScienceDirect

Composites Communications

journal homepage: www.elsevier.com/locate/coco

Short communication

On the mix-mode fracture of carbon fibre/epoxy composites interleaved with various thermoplastic veils

Dong Quan [a,b], Dongsheng Yue [a], Yannan Ma [a], Guoqun Zhao [a,*], René Alderliesten [b,*]

[a] Key Laboratory for Liquid–Solid Structural Evolution and Processing of Materials (Ministry of Education), Shandong University, China
[b] Structural Integrity & Composites Group, Delft University of Technology, Netherlands

ARTICLE INFO

Keywords:
Carbon fibre/epoxy composite
Interlayer toughening
Thermoplastic veils
Mix mode-I/II fracture

ABSTRACT

This work studied the mix mode-I/II fracture behaviour of an aerospace-grade carbon fibre/epoxy composite that was interlayer-toughened by Polyamide-12 (PA), Polyphenylene-sulphide (PPS), Polyimide (PI), Polyethersulfone (PES) and Polyethylenimine (PEI) fibres. During the laminate curing process, the PA fibres melted, the PPS and PI fibres kept in their original form and the PES and PEI fibres dissolved in the epoxy matrix. This resulted in different toughening mechanisms of the veils for the mix mode-I/II fracture of the laminates, which was studied using a cracked lap-shear test. The main toughening mechanisms were observed to be plastic deformation and failure of the thermoplastic resin for the meltable PA veils, thermoplastic fibre debonding and bridging for the intact PPS and PI veils, and thermoplastic particle debonding and plastic void growth for the dissolvable PES and PEI veils. The experimental results revealed that the fibre debonding and bridging mechanism was superior for toughness enhancement, followed by the thermoplastic particle debonding and plastic void growth mechanism. For instance, interleaving the PPS and PEI veils increased the mix-mode fracture propagation energy of the laminates by 345% and 171%, respectively. However, the toughening performance of the PA and PI veils was poor, since the crack mainly propagated at the vicinity around the interlayer/laminate interface.

1. Introduction

Interlayer toughening is an attractive method to enhance the interlaminar fracture properties of carbon fibre/epoxy composites. To date, many different types of materials have been employed as interlayers for laminate toughening, including cellulose fibres [1,2], thermoplastic fibres [3,4] and carbon nano-materials [5,6]. Among them, non-woven veils based on nano-/micro-scale thermoplastic fibres had proved outstanding performance [4,7] for laminate toughening, without causing significant drops in the mechanical properties and increases in the laminate weight [8]. Accordingly, the usage of thermoplastic veils for interlayer toughening of composites has attracted considerable attention of researchers and industrialists.

Veils based on various thermoplastic fibres, including Polyamide-12 (PA), Polyethersulfone (PES), Polyethylenimine (PEI), Polyphenylene-sulphide (PPS), Polyvinylidene fluoride (PVDF) and Polyvinyl-alcohol (PVA) had been utilised for interlayer toughening [8], with different levels of toughness improvements being achieved. Depending on the materials of the veils and the laminate curing schedules, three different types of interactions between the veils and the epoxy matrix can take place during the laminate curing process, i.e. the thermoplastic fibres melted, remained in their original forms and dissolved in the epoxy matrix [4,9,10]. This subsequently affected the forms of the thermoplastic veils in the cured laminates and influenced their toughening mechanisms and performance. Accordingly, it is necessary to compare the toughening performance of different forms of thermoplastic veils. Moreover, the majority of the relevant literature focused on the pure mode-I and mode-II fracture behaviour of the interleaved laminates, while the composite structures are mainly loaded under mix mode-I/II conditions in aerospace applications. For these reasons, this work aimed to study the mix mode-I/II fracture behaviour of carbon fibre/epoxy composites that were interlayer-toughened by different thermoplastic veils. In specific, an aerospace-grade carbon fibre/epoxy composite was interleaved with thermoplastic veils based on PA, PPS, PI, PES and PEI fibres. During the laminate curing process, the PA fibres melted, the PPS and PI fibres remained in their original forms and the PES and PEI fibres dissolved in the epoxy matrix of the laminate. The toughening performance and mechanisms of these thermoplastic veils on the mix mode-I/II fracture behaviour of the laminates had been investigated.

* Corresponding authors.
E-mail addresses: quandong@sdu.edu.cn (G. Zhao), R.C.Alderliesten@tudelft.nl (R. Alderliesten).

https://doi.org/10.1016/j.coco.2022.101230
Received 2 May 2022; Received in revised form 13 June 2022; Accepted 15 June 2022
Available online 21 June 2022

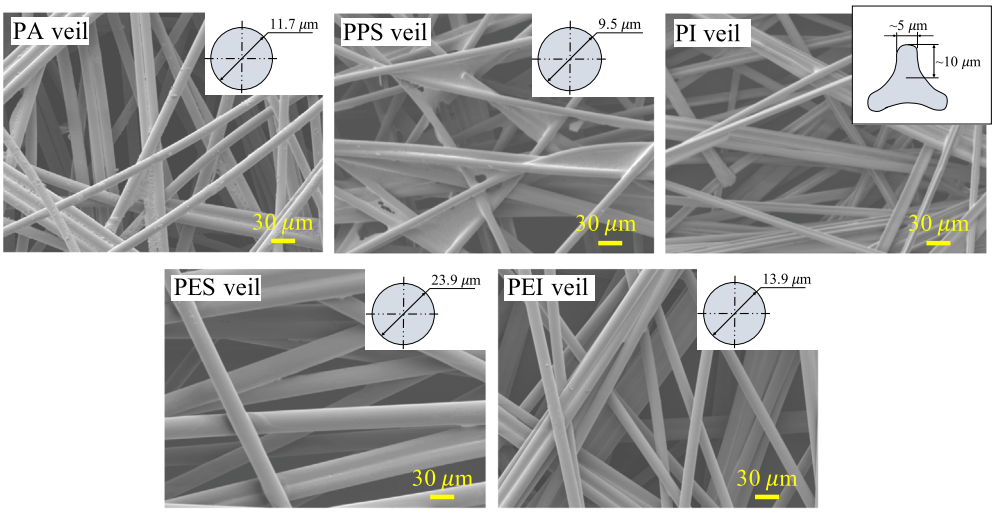

Fig. 1. Microscopy images of the thermoplastic veils. The inset images show the shape and dimension of the cross sections of the fibres.

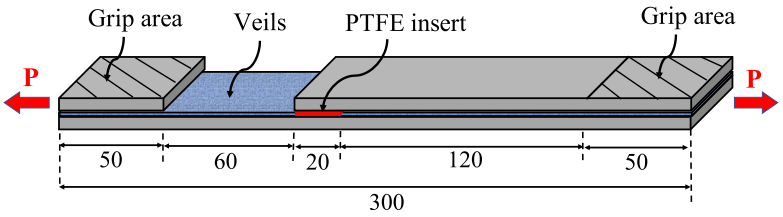

Fig. 2. Illustration of the CLS tests. The unit is mm.

Table 1
The mechanical and physical properties of the thermoplastic fibres.

Items	PA	PPS	PI	PES	PEI
tensile modulus [GPa]	1.4	3.8	3.6	2.7	3.0
tensile strength [MPa]	45	90	140	90	105
density [g/cm^3]	1.01	1.30	1.41	1.35	1.27
fibre length [mm]	10	10	10	10	10

2. Experimental

2.1. Materials and sample preparation

The unidirectional carbon fibre/epoxy prepreg was HexPly 8552-IM7-35%-134 from Hexcel. The thermoplastic veils based on PA, PPS, PI, PES and PEI fibres were supplied by Technical Fibre Products Ltd. (UK). The areal density of all the thermoplastic veils was 20 g/m^2. Fig. 1 shows typical microscopy images of the thermoplastic veils. The PA, PPS, PES and PEI fibres possessed a circular cross-section, and the PI fibres had a trilobal cross-section. The fibre diameters were measured to be 11.7 ± 1.5 μm, 9.5 ± 1.1 μm, 23.9 ± 2.6 μm and 13.9 ± 0.9 μm for the PA, PPS, PES and PEI fibres, respectively. The thickness of the blade of the trilobal PI fibre was around 5 μm, and the distance between the centre of the pivot and the edge of the blade was around 10 μm, as shown by the inset image in Fig. 1. Additional information about the mechanical and physical properties of the thermoplastic fibres can be found in Table 1.

The mix-mode fracture behaviour of the interleaved laminates was evaluated by a cracked lap shear (CLS) test, as schematically shown in Fig. 2. This test method was chosen as it represents more realistically the loading experienced by an airplane wing, that was studied in-depth by Bombardier Aerospace. The mode-mixity of the CLS tests, i.e. mode-I/mode-II was determined to be 26%/73% by a combined numerical and experimental study [11]. To prepare the CLS specimens, the layups for both of the strap and the lap substrate were prepared by stacking 20 layers of unidirectional prepregs together, with a 10 min de-bulking process being applied between every fourth layer at an under pressure lower than 100 mbar. The layups were then assembled together with a layer of thermoplastic veil being placed in between. A piece of PTFE film with a thickness of 13 μm was also placed at the mid-plane for generating a crack starter with a length of 20 mm. A layup consisting of 20 layers of unidirectional prepregs was also assembled to the panels to obtain the grip-area at the left end of the CLS specimen in Fig. 2. The laminate assemble was then cured at 185 °C and 6 bar pressure for 120 min in the autoclave. A vacuum pressure of 200 mbar inside the vacuum bag was used throughout the curing process. After the curing, the laminates were machined into desired dimensions as specified in Fig. 2.

2.2. Testing and analysis

The CLS test was carried out on a Zwick-Roll testing machine at a constant displacement rate of 0.2 mm/min. During the testing, a high resolution digital camera was used to monitor the crack length at one side of the specimen, that was synchronised with the load and displacement measurement based on the start time of the test. A pre-crack with a 5 mm length from the crack starter was generated by opening the specimens with a razor blade. Four replicate tests were conducted in each case. The mix-mode fracture energy of the laminates was calculated based on the equation given by Brussat et al. [12]:

$$G_T = \frac{P^2}{2b(EA)_2}\left[1 - \frac{(EA)_2}{(EA)_0}\right] \quad (1)$$

where G_T is the total fracture energy of a CLS specimen, P is the load applied, b is the width of the CLS specimen, E is the Young's modulus, A is the cross-section area, $(EA)_2$ is the tensile rigidity of the strap and $(EA)_0$ is the tensile rigidity of the overall structure.

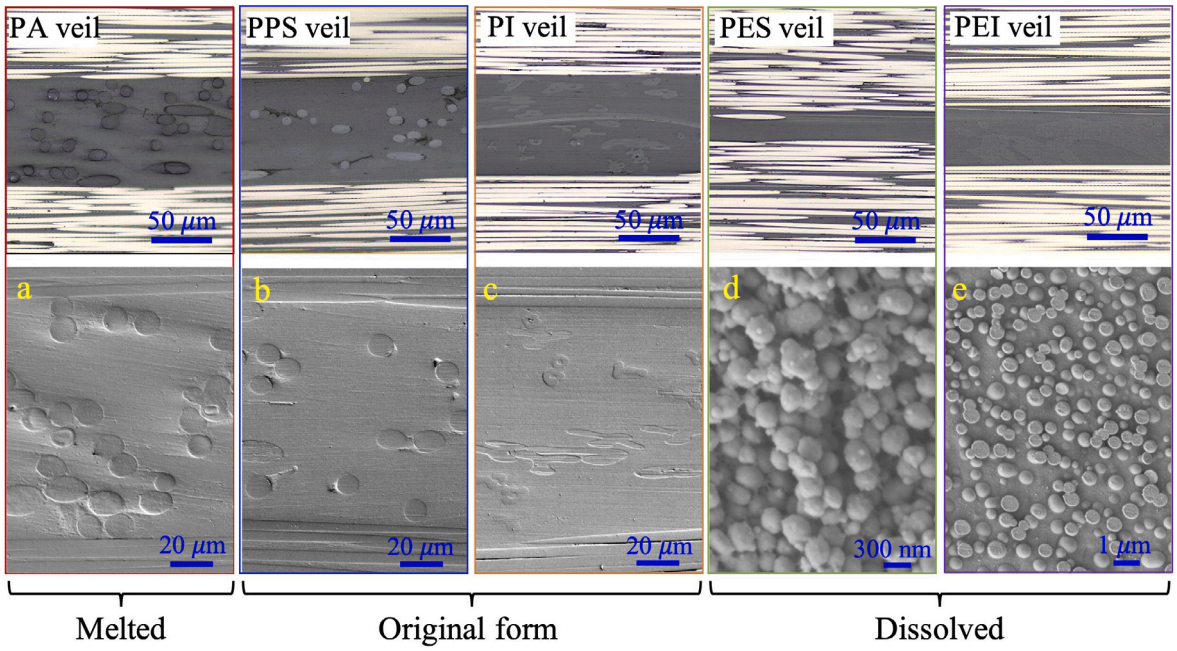

Fig. 3. Side-view images of the interlayers in the laminates.

To study the morphology of the thermoplastic veils in the laminates and the toughening mechanisms of the veils, the cross section of the interleaved laminates and the fracture surfaces of the CLS specimens were analysed using a VK-X1000 microscope from KEYENCE Corporation and a scanning electron microscope (SEM, JOEL JSM-7500F).

3. Results and discussion

3.1. Morphology of the interlayers

Fig. 3 shows microscopy images of the cross sections of the interleaved laminates, with a focus on the interlayer region. The cross-sections of the samples were polished and then etched by 1 ml of N-Methyl-2-pyrrolidone (NMP) to provide a better contrast for the imaging. The melting temperature of the PA and PPS veils was measured to be 180 °C and 290 °C in the previous study [4], while the PI veils possessed a much better thermal resistance than the PPS veils showing no obvious melting temperature. Accordingly, the PA fibres melted during the laminate curing process at 185 °C, and the PPS and PI fibres remained in their original forms. Additionally, Fig. 3 (a) showed that the PA fibres kept in a fibrous form within the cured laminates. This means no mixture between the melted PA fibres and the epoxy matrix took place during the curing process. The PES and PEI veils possessed a high miscibility with the epoxy matrix of the laminates. They dissolved into the epoxy matrix during the curing process, and formed numerous thermoplastic particles in the interlayers, see Fig. 3 (d) and (e) [10,13]. It was also observed that the particle size of the PES was much smaller than the PEI within the cured laminates. This was because of the PES polymer possessed a higher solubility with the epoxy than the PEI polymer [14]. Moreover, no void was observed in the interlayers in all the cases, indicating a thorough impregnation of the thermoplastic veils by the epoxy matrix of the laminates. The thickness of the interlayers was measured to be 113.8 ± 1.7 μm,112.3 ± 3.8 μm,100.3 ± 2.2 μm, 20.7 ± 1.5 μm, 61.3 ± 1.5 μm for the PA, PPS, PI, PES and PEI veils, respectively. The thicknesses of the PES and PEI interlayers were much smaller than the other ones, owing to the dissolution of the PES and PEI veils.

3.2. Mix mode-I/II fracture of the interleaved laminates

Fig. 4 presents typical load versus displacement curves and corresponding *R*-curves from the CLS tests. The reference means the laminate without any interlayer. The curves for the interleaved laminates in Fig. 4 (a) were shifted to the right for easy observations. The circle points indicate where the crack lengths were recorded.

It was observed that the fracture loads of the laminates had been increased to different levels by adding various thermoplastic veils except the PI one. Among all the different interlayers, the addition of PPS veils almost doubled the fracture loads of the laminates, as shown in Fig. 4 (a). Consequently, the addition of PI veils led to a slight drop in the *R*-curve, while incorporating all the other veils caused an increase in the *R*-curves of the laminates, see Fig. 4 (b). It should be noted that the PPS interleaved laminate failed dynamically after the crack steadily propagated to a crack length of approximately 60 mm. This typically indicated a significant extension in the length of the fracture damage zone ahead of the crack tip [15], that was always associated with a relatively high fracture toughness. The fracture initiation energy (G_T^{ini}) and fracture propagation energy (G_T^{prop}) of the interleaved laminates were summarised in Table 2. The values of G_T^{prop} were calculated by averaging all the values above a crack length of 40 mm on the *R*-curves in Fig. 4 (b). It was found that interleaving the PI veils slightly decreased G_T^{ini} and G_T^{prop} of the laminate by 22% and 4%, respectively, while the addition of all the other interlayers increased the fracture energies of the laminates by different extents. In specific, the most significant improvement in the fracture toughness was obtained by interleaving the PPS veils, i.e. an increase of 134% and 345% was obtained for G_T^{ini} and G_T^{prop}, respectively. The dissolvable PEI veils ranked second for the toughness enhancement, and it significantly increased G_T^{ini} and G_T^{prop} by 92% and 171%, respectively. Additionally, the incorporation of meltable PA veils had negligible effect on G_T^{ini}, but increased G_T^{prop} by 56%.

Fig. 5 shows side-view images of the tested CLS specimens for showing their crack paths, and typical SEM images of the corresponding fracture surfaces. From Fig. 5 (a), it was found that the crack propagated at the vicinity of the interlayer/carbon fibre interface for the laminate interleaved with the meltable PA veils, leaving almost the entire interlayers on the bottom side of the fracture surfaces. This type of failure mode was caused by a good adhesion between the melting

Table 2
The fracture initiation energy (G_T^{ini}) and fracture propagation energy (G_T^{prop}) of the interleaved laminates. The values in the brackets indicate the percentage increases when compared to the reference laminate.

Items	Reference	PA	PPS	PI	PES	PEI
G_T^{ini} (J/m^2)	549 ± 85 *	549 ± 89 (+0%)	1284 ± 158 (+134%)	427 ± 45 (-22%)	788 ± 67 (+44%)	1053 ± 124 (+92%)
G_T^{prop} (J/m^2)	627 ± 94 *	855 ± 193 (+56%)	2441 ± 87 (+345%)	530 ± 133 (-4%)	997 ± 21 (+82%)	1490 ± 83 (+171%)

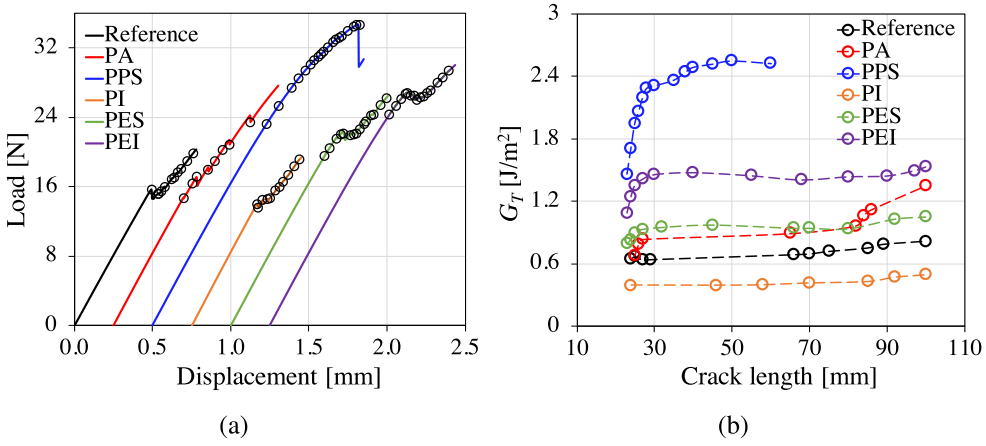

Fig. 4. The load versus displacement curves and corresponding *R* curves from the CLS tests. The curves for the interleaved laminates in (a) were shifted to the right for easy observations. The circle points indicate where the crack lengths were monitored.

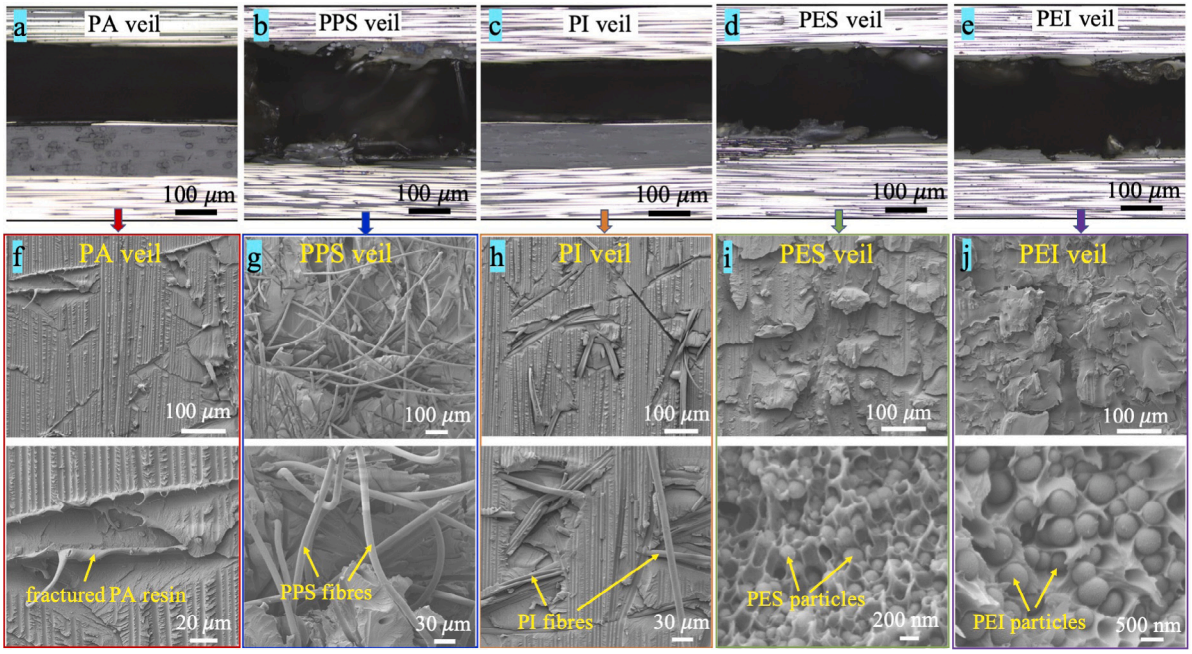

Fig. 5. Side-view images of the tested CLS specimens for showing their crack paths (a–e), and typical SEM images of the corresponding fracture surfaces (f–j).

PA veils and the laminate epoxy matrix, that prevented the crack to migrate into the interlayers [7]. Moreover, the main failure mechanism of the melted PA fibres was observed to be plastic deformation and failure of the PA resin, as shown in Fig. 5(f). However, only a very limited number of PA fibres got involved in the fracture process of the laminate due to the interlayer/carbon fibre interface failure. This resulted in the relatively poor toughening performance of the PA veils, as shown in Table 2. Similarly, the fracture also took place at the interlayer/carbon fibre interface for the PI-interleaved laminate (as shown in Fig. 5(c)), leaving the majority of the PI fibres embedded in the interlayer without making any contribution to the fracture toughness (see Fig. 5(h)). The laminates interleaved with the PPS, PES and PEI veils exhibited a cohesive failure within the interlayers, as shown in Fig. 5(b), (d) and (e). For the PPS-interleaved laminates, numerous PPS fibres were observed on the fracture surfaces (see Fig. 5(g)). This means the main toughening mechanism of the PPS veils was PPS fibre debonding and bridging during the fracture process. For the laminates interleaved with the dissolvable PES and PEI veils, the fracture surfaces were covered with a layer of fractured interlayers, that contained numerous thermoplastic particles (see Fig. 5(i) and (j)). These phenomena indicate that the main toughening mechanism of the PES and PEI veils was the debonding of the thermoplastic particles, that

was typically followed by plastic void growth and shear band yielding of the surrounding epoxy matrix. Based on the above observations, it is clear that a cohesive failure in the interlayers was necessary to obtain good toughening effectiveness, and thermoplastic fibre debonding and bridging was the most effective mechanism for toughness improvement.

4. Conclusions

Thermoplastic veils based on PA, PPS, PI, PES and PEI fibres were used for interlayer toughening of an aerospace-grade carbon fibre/epoxy composites. During the laminate curing process, the PA fibres melted, the PPS and PI fibres kept in their original form and the PES and PEI fibres dissolved in the epoxy matrix of the laminates. The experimental results of the cracked lap-shear tests demonstrated that the fracture toughness and toughening mechanisms were determined by the forms of the thermoplastic veils in the cured laminates and the location of the fracture path during the fracture process. The toughening performance of the thermoplastic veils was poor for the PA and PI veils. This was because of the fracture propagated around the interface between the laminate and the interlayers, in which case, the toughening mechanisms of the PA and PI interlayers were not activated. The dissolvable PES and PEI veils exhibited good toughening effectiveness by introducing numerous toughening thermoplastic particles in the interlayers. For example, interleaving the PEI veils increased the mix-mode fracture initiation energy and propagation energy of the laminate by 92% and 171%, respectively. The most effective toughening mechanism was observed to be the fibre debonding and bridging mechanism of the PPS veils, that significantly improved the mix-mode fracture initiation energy and propagation energy of the laminate by 134% and 345%, respectively.

CRediT authorship contribution statement

Dong Quan: Conceptualization, Investigation, Funding acquisition, Writing – original draft. **Dongsheng Yue:** Methodology, Investigation. **Yannan Ma:** Methodology, Investigation. **Guoqun Zhao:** Project administration, Funding acquisition, Writing – review & editing. **René Alderliesten:** Conceptualization, Writing – review & editing.

Declaration of competing interest

The authors declare that they have no known competing financial interests or personal relationships that could have appeared to influence the work reported in this paper.

Data availability

Data will be made available on request.

Acknowledgements

The authors would like to acknowledge the financial support from Natural Science Foundation of Shandong Province (Grant No. : 2022 HWYQ-013), the key research and development program of Shandong Province (Grant No. 2021ZLGX01), and Qilu Young Scholar Program of Shandong University (Grant No.: 31370082163164). We acknowledge Bombardier Aerospace (Belfast) and Technical Fibre Products (UK) for supplying the carbon fibre composites and thermoplastic veils employed in this study.

References

[1] Z. Zhang, K. Fu, Y. Li, Improved interlaminar fracture toughness of carbon fiber/epoxy composites with a multiscale cellulose fiber interlayer, Compos. Commun. 27 (2021) 100898, http://dx.doi.org/10.1016/j.coco.2021.100898.

[2] X. Zhu, Y. Li, T. Yu, Z. Zhang, Enhancement of the interlaminar fracture toughness and damping properties of carbon fiber reinforced composites using cellulose nanofiber interleaves, Compos. Commun. 28 (2021) 100940, http://dx.doi.org/10.1016/j.coco.2021.100940.

[3] X. Song, J. Gao, N. Zheng, H. Zhou, Y.-W. Mai, Interlaminar toughening in carbon fiber/epoxy composites interleaved with CNT-decorated polycaprolactone nanofibers, Compos. Commun. 24 (2021) 100622, http://dx.doi.org/10.1016/j.coco.2020.100622.

[4] D. Quan, F. Bologna, G. Scarselli, A. Ivankovic, N. Murphy, Interlaminar fracture toughness of aerospace-grade carbon fibre reinforced plastics interleaved with thermoplastic veils, Composites A 128 (2020) 105642, http://dx.doi.org/10.1016/j.compositesa.2019.105642.

[5] S. Patnaik, P.K. Gangineni, R.K. Prusty, Influence of cryogenic temperature on mechanical behavior of graphene carboxyl grafted carbon fiber reinforced polymer composites: An emphasis on concentration of nanofillers, Compos. Commun. 20 (2020) 100369, http://dx.doi.org/10.1016/j.coco.2020.100369.

[6] C.-Y. Dang, K. Liu, M.-X. Fan, S.-Q. Zhu, S.-H. Zhao, X.-J. Shen, Investigation on cryogenic interlaminar shear properties of carbon fabric/epoxy composites improved by graphene oxide-coated glass fibers, Compos. Commun. 22 (2020) 100510, http://dx.doi.org/10.1016/j.coco.2020.100510.

[7] D. Quan, R. Alderliesten, C. Dransfeld, N. Murphy, A. Ivankovic, R. Benedictus, Enhancing the fracture toughness of carbon fibre/epoxy composites by interleaving hybrid meltable/non-meltable thermoplastic veils, Compos. Struct. 252 (2020) 112699, http://dx.doi.org/10.1016/j.compstruct.2020.112699.

[8] R. Palazzetti, A. Zucchelli, Electrospun nanofibers as reinforcement for composite laminates materials - a review, Compos. Struct. 182 (2017) 711–727, http://dx.doi.org/10.1016/j.compstruct.2017.09.021.

[9] V.A. Ramirez, P.J. Hogg, W.W. Sampson, The influence of the nonwoven veil architectures on interlaminar fracture toughness of interleaved composites, Compos. Sci. Technol. 110 (2015) 103–110, http://dx.doi.org/10.1016/j.compscitech.2015.01.016.

[10] C. Cheng, Z. Chen, Z. Huang, C. Zhang, R. Tusiime, J. Zhou, Z. Sun, Y. Liu, M. Yu, H. Zhang, Simultaneously improving mode I and mode II fracture toughness of the carbon fiber/epoxy composite laminates via interleaved with uniformly aligned PES fiber webs, Composites A 129 (2020) 105696, http://dx.doi.org/10.1016/j.compositesa.2019.105696.

[11] L. Binsfeld, The Conceptual Design, Development, Testing and Modelling of Spotscrew Enhanced Co-Injected/co-Cured Joints in Aerospace-Grade Composites (Ph.D. thesis), University College Dublin, 2020.

[12] T. Brussat, S. Chiu, S. Mostovoy, Fracture Mechanics for Structure Adhesive Bonds - Final Report, Technical Reeport, 1997.

[13] Z. Chen, J. Luo, Z. Huang, C. Cai, R. Tusiime, Z. Li, H. Wang, C. Cheng, Y. Liu, Z. Sun, H. Zhang, J. Yu, Synergistic toughen epoxy resin by incorporation of polyetherimide and amino groups grafted MWCNTs, Compos. Commun. 21 (2020) 100377, http://dx.doi.org/10.1016/j.coco.2020.100377.

[14] C. Hansen, Hansen Solubility Parameters: A User's Handbook, CRC Press, Fla, 2000.

[15] D. Quan, J.L. Urdaniz, A. Ivankovic, Enhancing mode-I and mode-II fracture toughness of epoxy and carbon fibre reinforced epoxy composites using multi-walled carbon nanotubes, Mater. Des. 143 (2018) 81–92, http://dx.doi.org/10.1016/j.matdes.2018.01.051.